2008

An Efficient Network Model for Determining the Effective Thermal Conductivity of Particulate Thermal Interface Materials

S Kanuparthi

G Subbarayan

Thomas Siegmund
Purdue University, siegmund@purdue.edu

B Sammakia

An Efficient Network Model for Determining the Effective Thermal Conductivity of Particulate Thermal Interface Materials

S. Kanuparthi[1], G. Subbarayan[1+], T. Siegmund[1] and B. Sammakia[2]

[1]School of Mechanical Engineering, Purdue University, West Lafayette, IN 47906

[2]Watson School of Engineering, State University of New York, Binghamton, NY 13902

[+] Tel: (765) 494-9770 Email: ganeshs@purdue.edu

Manuscript ID: **TCPT-2007-004.R1**

Abstract

Particulate composites are commonly used in Microelectronics applications. One example of such materials is Thermal Interface Materials (TIMs) that are used to reduce the contact resistance between the chip and the heat sink. The existing analytical descriptions of thermal transport in particulate systems do not accurately account for the effect of inter-particle interactions, especially in the intermediate volume fractions of 30-80%. Another crucial drawback in the existing analytical as well as the network models is the inability to model size distributions (typically bimodal) of the filler material particles that are obtained as a result of the material manufacturing process. While full-field simulations (using, for instance, the finite element method) are possible for such systems, they are computationally expensive. In the present paper, we develop an efficient network model that captures the physics of inter-particle interactions and allows for random size distributions. Twenty random microstructural arrangements each of Alumina as well as Silver particles in Silicone and Epoxy matrices were generated using an algorithm implemented using a java language code. The microstructures were evaluated through both full-field simulations as well as the network model. The full-field simulations were carried out using a novel meshless analysis technique developed in the author's (GS) research [26]. In all cases, it is shown that the random network models are accurate to within 5% of the full field simulations. The random network model simulations were efficient since they required two orders of magnitude smaller computation time to complete in comparison to the full field simulation.

Keywords: Thermal interface materials, network models, full-field simulations.

Nomenclature

k_{eff} effective thermal conductivity of the composite, [W/mK]

k_m thermal conductivity of the base (polymer) matrix, [W/mK]

k_p thermal conductivity of the filler material particles, [W/mK]

k thermal conductivity of rectangular bar, [W/mK]

A cross-sectional area of the rectangular bar, [m^2]

l length of the rectangular bar, [m]

q heat flowing to the respective node, [W]

R_b thermal interfacial boundary resistance, [Km^2/W]

K_1, K_2, K_3 conductances in series across two filler particles, [W/K]

K_{ij} effective conductance between particles "i" and "j", [W/K]

T temperature at the node, [K]

R_{12} radius of the cylindrical zone of thermal transport, [m]

R_1, R_2 radii of the spherical filler particles, [m]

a_{12} mean radius of the two spherical filler particles, [m]

h_{ij} minimum gap width between two spherical filler particles, [m]

d_i distance of the center of a filler particle from an interface, [m]

r nearest filler particle surface distance from an arbitrary point in the matrix, [m]

r_{avg} average radius of all the filler particles in the simulated microstructures, [m]

r_p radius of the filler particles, [m]

r_m mean radius of the filler particles in a microstructure, [m]

D average diameter of the filler particles in a microstructure, [m]

Greek symbols

ε, α non-dimensional parameters

η, θ Weibull-parameters

Δ nodal temperature difference between jNURBS and the RNM [K]

Subscripts

1, 2 and 3 filler particles

i, j filler particles

m matrix

p filler particle

eff effective or composite

b bottom interface

t top interface

Superscripts

- average quantities

Abréviations

TIM Thermal Interface Material

SC self-consistent

jNURBS java based meshfree full field simulation code

RVE Representative Volume Element

BAM Bruggeman Asymmetric Model

Introduction

Thermal Interface Materials (TIMs) are widely used in the microelectronics industry to effectively expel the waste heat generated in the chips. They provide a conducting layer that reduces the thermal resistance between the chip and the heat sink. A critical need in developing these TIMs is apriori modeling using fundamental physical principles to predict the effect of particle volume fraction and arrangements on effective behavior. Such models will enable one to optimize the structure and arrangement of the material. The analytical descriptions of thermal transport in particulate systems are mostly inspired by the pioneering work of Maxwell [1] and Rayleigh [2]. The effective medium approximations for evaluating the effective thermal conductivity of particulate composites can be broadly classified as [3]: i) Maxwell's approximation based models, ii) Self-consistent models, and iii) Differential effective medium models. The Maxwell's model and its derivatives describe arrangement of particles at dilute concentrations by modeling one particle embedded in a matrix of infinite extent. Rayleigh [2] developed a solution for the effective behavior of a system in which the inclusions were arranged periodically. Therefore, in Rayleigh's model, the inter-particle interactions are considered by assuming that the particles conform to a simple cubic arrangement. Extensions to Rayleigh's model include those that have allowed other alternative periodic arrangements (to the simple cubic arrangement) such as face-centered cubic and body-centered cubic cells [4, 5] as well as those that have studied the effective behavior of particles in near contact [6]. There is an inherent assumption of the spheres being "well separated" from one another in these models as well [3].

The extensions to Maxwell's model include those that have introduced imperfect interfacial contact [7] as well as those that have modeled non-spherical particles [8]. Benvensite [9] obtained the same result as Hasselman et al. [7] based on a micromechanics (Mori-Tanaka based) approach. These models are applicable only at dilute concentrations, when the inclusions are well separated from one-another. Another drawback in the above models is that they do not account for the random size distribution or the polydispersivity of the inclusions. The effective thermal conductivity of particulate composites in general depends on the degree of polydispersivity of the inclusions [3].

Another popular method of estimating the effective thermal conductivity of composites is using the self-consistent (SC) approximation, which was originally developed by Bruggeman [10] and further extended by Landauer [11, 12]. The method is based on the approximation that the medium outside a particular type of inclusion can be considered to be homogeneous, the effective conductivity of which needs to be determined. SC approximations do not account for the spatial distribution of the inclusions and are of questionable validity when applied to systems that do not posses phase-inversion symmetry [3]. The fundamental assumption of the existence of an effective medium outside of a "test" sphere is invalid when identical spheres are packed. The SC approximation also fails when applied to composites with widely different phase thermal conductivities [3].

The asymmetric differential effective-medium approximation scheme was also developed by Bruggeman [10]. Bruggeman assumed that the filler material particles were added progressively to a composite matrix whose effective behavior is known at any given stage. Every et al. [13] used Bruggeman's asymmetric model (BAM) for predicting

the effective thermal conductivity of ZnS/Diamond composites. The deficiencies of using the BAM for predicting the composite thermal conductivity are described in [14].

In Figure 1, a comparison of the experimental results against the prediction by Maxwell's model, Rayleigh's model and BAM model (assuming thermal interfacial boundary resistance, R_b, to be equal to zero) is shown. The matrix considered here is Silicone (k_m = 0.2 W/mK) and the filler particles are Alumina (k_p = 25 W/mK). The size distribution of the Alumina fillers ranged from a few nanometers to 20 microns (with a mean size of 7.99 μm). The size distributions of the filler particles were obtained using a particle size distribution analyzer at General Electric Company – Global Research Center, Niskayuna, New York and are shown below in Figure 2. The instrument was incapable of detecting particles smaller than 400 nanometers. The Hashin-Shtrikman bounds [3] are also shown in the figure for comparison. The details behind the experimental characterization are provided elsewhere [15].

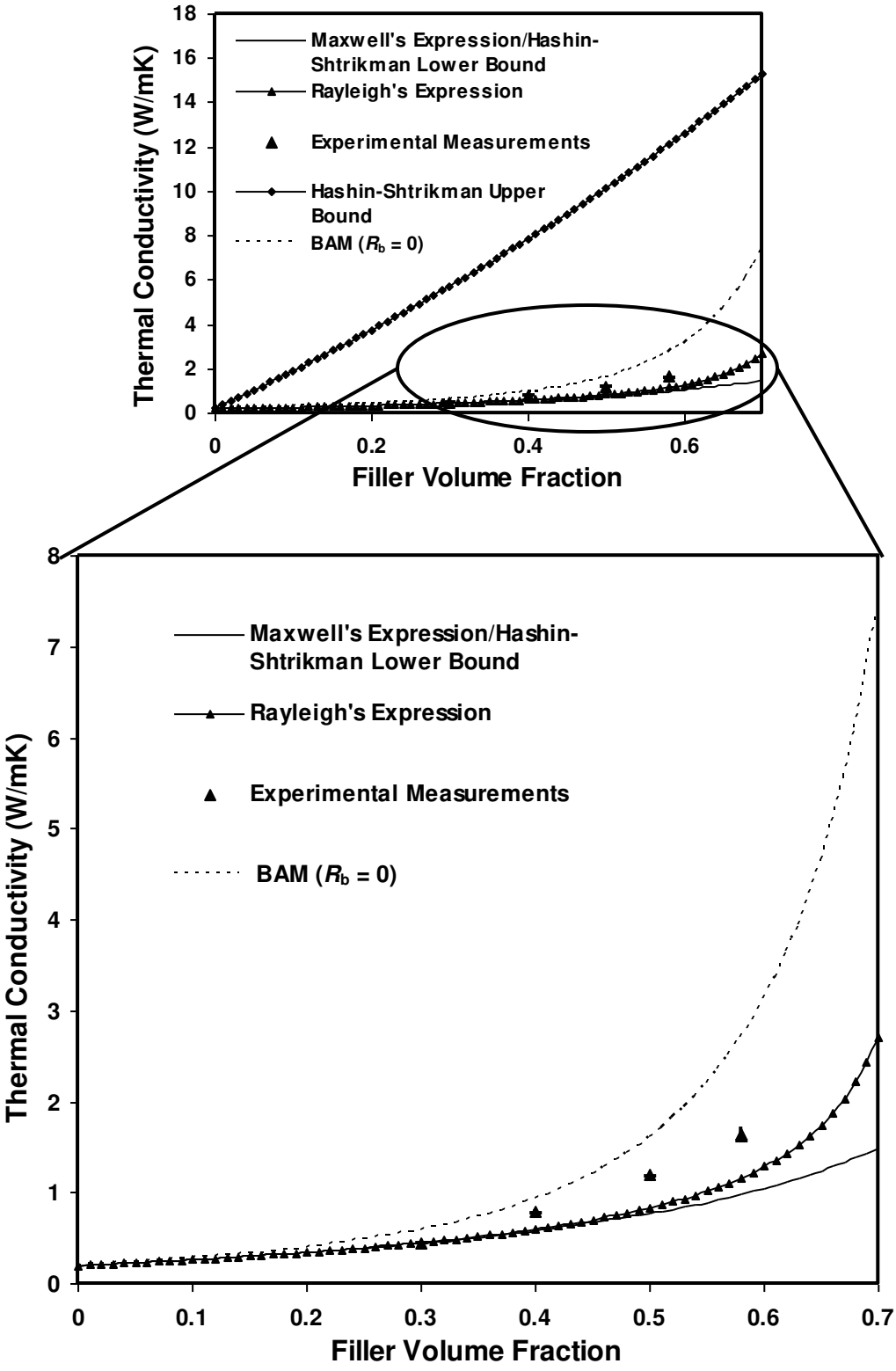

Figure 1: Alumina filler particles in Silicone matrix: Comparison of analytical models against experimental measurements.

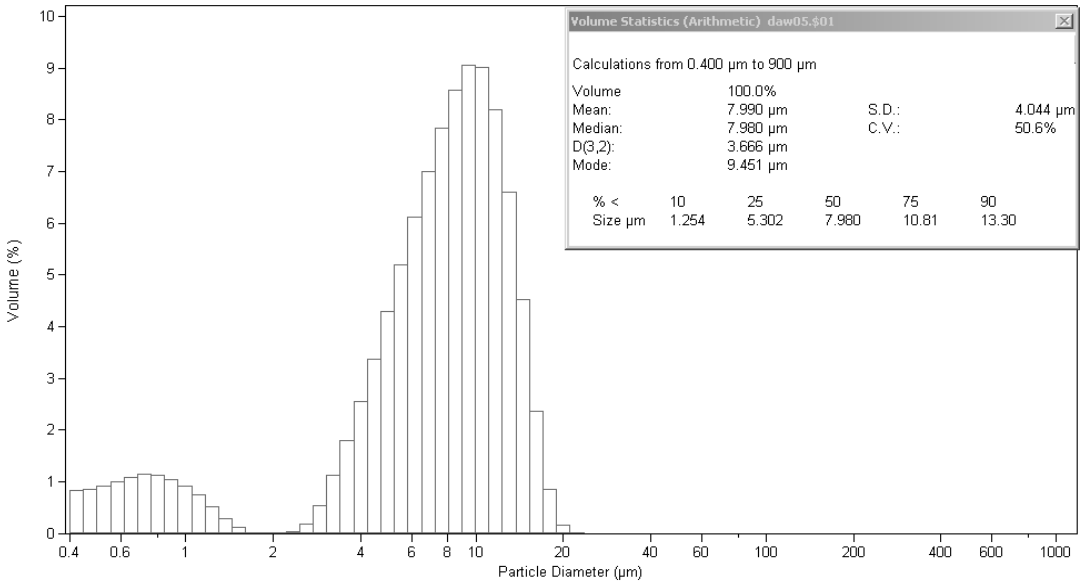

Figure 2: Size distribution of the Alumina filler particles used in the experiments.

As can be seen from Figure 1, most classical theories are observed to be accurate at dilute concentrations when filler material volume fractions are less than 30-35%, but they are often inaccurate at larger volume fractions and when particles are in "near percolation" arrangements. Volume loadings of particles are typically in the 60-70% range for thermal interface materials. For high volume loading of filler particles, the Maxwell and Rayleigh models' predictions are lower in comparison to the experimental measurements while BAM model's predictions are higher when compared to the experimental measurements.

In the present paper, a random network model that includes the physics of inter-particle interaction is developed for TIM systems. The developed numerical procedure is intended as an accurate alternative to both analytical derivations as well as simple network based percolation models that presume uniform particle sizes and regular

arrangement of particles on a grid. The simulations presented here possess the advantage of being more accurate compared with the analytical models at higher volume loading due to their ability to capture inter-particle interaction. They have the advantage of being able to handle random particle size variations compared to the network based percolation models [16, 17 and 18] as they are commonly used. The common network based percolation models approximate flux paths through orthogonal resistance networks, which may also limit their accuracy. The numerical simulations of the present study do not make this assumption. The numerical simulations presented here are also demonstrated to be accurate and very efficient in predicting the bulk thermal conductivity of the TIM composites in comparison to the full-field, explicit numerical simulations of particle arrangements [19, 20]. These characteristics are believed to make the numerical simulations presented here an accurate and efficient alternative to currently existing analytical and numerical approaches.

Microstructure Generation and Characterization

We begin the development of the methodology with a description of the procedure to generate random microstructures representative of particulate TIMs. To achieve maximally packed microstructures for a given distribution of particles, the drop-fall-shake algorithm [21] and references there within as well as [25] was implemented. This algorithm was modified to generate microstructures that are not maximally packed, but corresponding to a given volume fraction. That is, the random initial arrangement without further execution of the drop-fall-shake algorithm led to microstructures of a prescribed volume fraction. The algorithm is pictorially illustrated in Figure 3 and an example microstructure corresponding to 58% particle loading is illustrated in Figure 4.

The algorithm was implemented in a Java language code. The generated microstructures were also statistically described using the matrix nearest exclusion probability function [3], which is described in detail below. The code was used to generate approximately forty such random microstructures (similar to those shown in Figure 4) in one hour on a 3 GHz Pentium 4 machine with 1GB RAM.

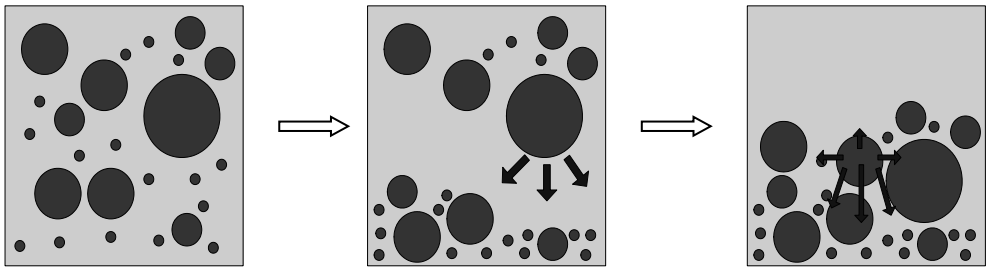

Figure 3: Generating a random dense microstructure: drop-fall-shake algorithm.

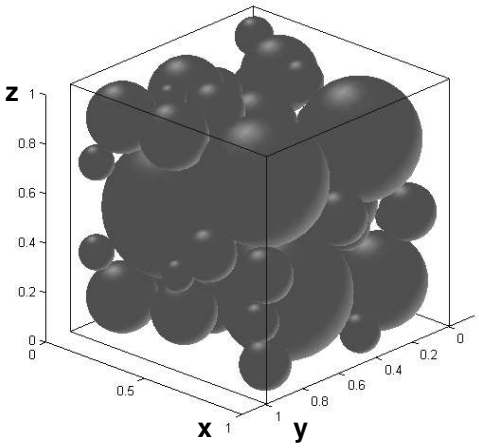

Figure 4: Random microstructure RVE of the thermal interface material.

There are well established mathematical formalisms for stochastically characterizing random microstructures [3]. In particular, for characterizing polydispersed systems, nearest-surface distribution functions are more relevant than the nearest-neighbor distribution functions [22]. The matrix nearest-surface distribution function

Manuscript ID: **TCPT-2007-004.R1**

$h_v(r)$ is defined such that $h_v(r)dr$ is the probability that the nearest particle surface lies at a distance between r and $r + dr$, from an arbitrary matrix point (points in the microstructure lying exterior to the particles in the matrix region) in the microstructure. The corresponding exclusion probability function $e_v(r)$ is associated with the complementary cumulative distribution function of $h_v(r)$ as:

$$e_v(r) = 1 - \int_{-\infty}^{r} h_v(x)dx \tag{1}$$

Twenty random microstructures with a 58% volume loading of fillers were generated using the above described procedure. The volume loading of the filler particles was fixed at 58%, so as to enable comparisons with experiments that were carried out at this volume loading. The normalized size of the simulated RVE's was considered to be 1 x 1 x 1 and the diameter of particles relative to the RVE side varied between 0.08 to 0.89 with a mean value of 0.25 and a standard deviation of 0.13. Random microstructures were simulated since the generation of microstructures with particle arrangements corresponding to the experimental conditions is a significant challenge as discussed in a later section of this paper. For example, to simulate the "exact" microstructures as that of the experiments for 58% volume loading of Alumina filler particles loaded in Silicone matrix (considering a unit cell whose sides are equal to five times the maximum particle diameter), the total number of particles that need to be simulated (based on the size distribution data shown in Figure 2) would be so large as to be computationally infeasible on desktop computers as shown in Table 1. Also, as the number of particles "n" simulated in the microstructure increases, the computational time for matrix inversion calculations in the random network model increases as a function of ~n^3.

Table 1: Estimated number of filler particles in a unit cell of size 95 μm x 95 μm x 95 μm.

Size (μm)	Vol %	# of Particles	Cumulative
0.5	3.56	315728	470150
0.7	3.46	111833	154422
0.9	1.86	28316	42589
1.1	0.86	7190	14273
1.3	0.66	3348	7083
2.765	0.22	114	3735
3.075	0.54	204	3621
3.38	1.13	323	3417
3.705	1.86	404	3094
4.055	2.59	430	2690
4.49	3.31	405	2260
5.02	4.22	369	1855
5.565	5.14	330	1486
6.18	6.04	283	1156
6.92	6.95	232	873
7.655	7.77	192	641
8.5	8.59	155	449
9.5	9.04	117	294
10.75	9.10	81	177
12.34	8.26	49	96
14.00	6.65	27	47
15.67	4.60	13	20
17.34	2.51	5	7
19	1.10	2	2

The matrix exclusion probability was evaluated by considering ~10^6 arbitrary matrix points for each of the microstructures. The matrix points were surrounded with concentric shells of radii $r_i = i\Delta r$, $i = 1,2,3.....$, and thickness Δr (where, $\Delta r << $ particle radii). For each matrix point, the particle that has the nearest surface distance was found and the corresponding distance was recorded. Subsequently, the number of shells (for a given shell radius r_i) containing the nearest surface points was counted. For a given shell radius, the number of successes divided by the total number of matrix points gives the probability $h_v(r)dr$ for that particular shell radius between r_i and $r_i + \Delta r$. From the $h_v(r)$

versus r plot, the matrix exclusion probability function $e_v(r)$ can be calculated using Equation (1) and multiplying it with the volume fraction of the matrix space in the microstructure. The probability plots for all the microstructures were generated and were fit using a Weibull distribution for the matrix nearest-surface distribution function $h_v(r)$ given by Equation (2):

$$h_v(r) = \eta\theta^{-\eta} r^{\eta-1} e^{-\left(\frac{r}{\theta}\right)^{\eta}} \qquad (2)$$

$$e_v(r) = e^{-\left(\frac{r}{\theta}\right)^{\eta}}$$

The mean and standard deviation of the Weibull parameters η and θ obtained from the plots were, $\overline{\eta}$ = 1.1472, σ_η = 0.0517 and $\overline{\theta}$ = 0.0381, σ_θ = 0.0029. The $e_v(r)$ characteristic of all the twenty, three-dimensional microstructures is shown in Figure 5. The three lines in the Figure 5 represent the values of $e_v(r)$ for ($\overline{\eta}$, $\overline{\theta}$), ($\overline{\eta}$ + 3σ_η, $\overline{\theta}$ + 3σ_θ) and ($\overline{\eta}$ - 3σ_η, $\overline{\theta}$ - 3σ_θ) respectively.

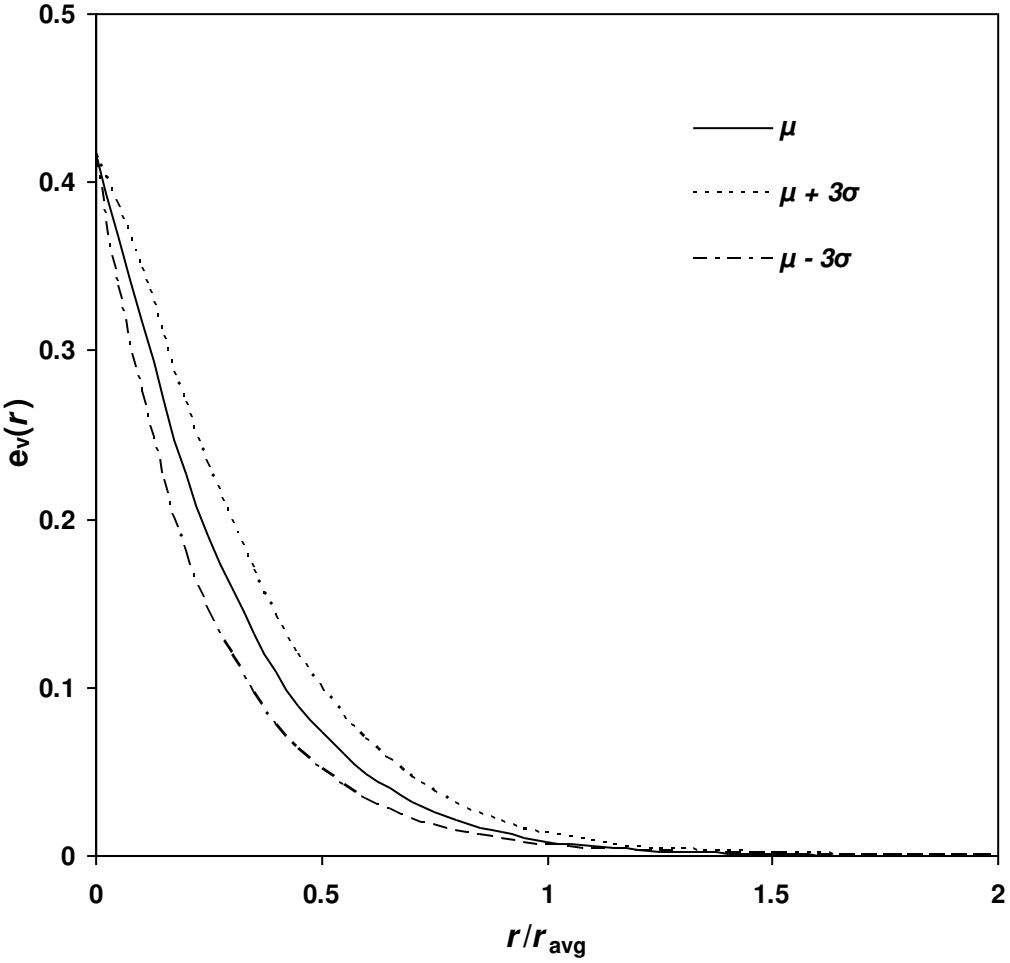

Figure 5: Characteristic matrix exclusion probability function $e_v(r)$ of the simulated microstructures. The volume loading of the filler particles in the microstructures is 58%.

The distance r in the above plot is rendered non-dimensional by the average radius r_{avg} of all the particles in all the twenty microstructures. From the above plot we can see that $e_v(0)$ is the volume fraction of the matrix phase in the microstructures, as expected.

Random Network Model Development

Considering one-dimensional heat transfer in a uniform bar of thermal conductivity k with a cross-sectional area A (perpendicular to the direction of heat transfer) and length l, the standard conductance matrix can be derived as:

$$\left(\frac{Ak}{l}\right)\begin{bmatrix} 1 & -1 \\ -1 & 1 \end{bmatrix}\begin{bmatrix} T_1 \\ T_2 \end{bmatrix} = -\begin{bmatrix} q_1 \\ q_2 \end{bmatrix} \tag{3}$$

where T_1 and T_2 represent the steady state temperatures at the two ends (nodes) of the uniform bar, and q_1 and q_2 represent the heat flowing to the nodes across which the one-dimensional bar element is connected. The term $(Ak)/l$ is the conductance K. When a particle-matrix type microstructure is modeled through a network of conductances there are at least two possible types of interactions that one must consider:

i. Particle–matrix–particle (Figure 6).

The equivalent conductance matrix for this situation is given by:

$$\begin{bmatrix} K_1 & -K_1 & 0 & 0 \\ -K_1 & K_1+K_2 & -K_2 & 0 \\ 0 & -K_2 & K_2+K_3 & -K_3 \\ 0 & 0 & -K_3 & K_3 \end{bmatrix}\begin{bmatrix} T_1 \\ T_2 \\ T_3 \\ T_4 \end{bmatrix} = -\begin{bmatrix} q_1 \\ q_2 \\ q_3 \\ q_4 \end{bmatrix} \tag{4}$$

where, K_1, K_2 and K_3 are the conductances within the particle 1, the matrix region and the particle 2, respectively, and T_1, T_2, T_3 and T_4 are the nodal temperatures as shown in Figure 6, and q_1, q_2, q_3 and q_4 represent the heat flowing to the respective nodes.

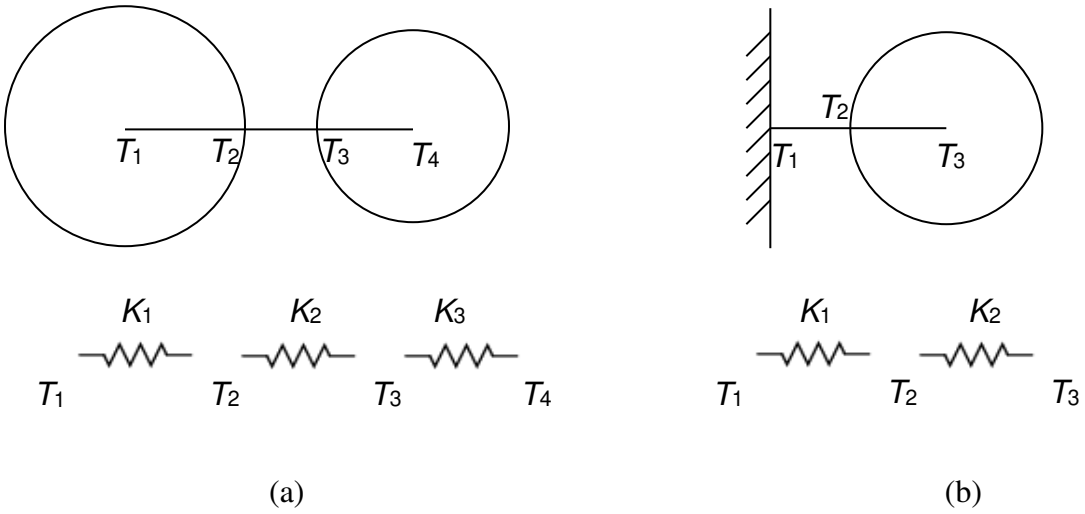

Figure 6: (a) Two filler particles in near-contact embedded in the matrix and the equivalent conductance network and (b) a particle near interface and its equivalent conductance network.

ii. Particle–matrix–substrate. The conductance matrix for this scenario is similar to that given in Equation (4).

In order to simulate the bulk TIM material, one needs to assemble the contributions of the above element conductance matrices into a global conductance matrix. The approach is to discretize the TIM system, place nodes at the centers of each of the filler particles, and evaluate the nodal temperatures by solving the global conductance matrix. Physically, this approach makes use of the fact that at *steady state,* net heat at each node must be equal to *zero*.

A Model for Inter-Particle Conductance

Batchelor et al. [23] proposed that the thermal flux density across the surface of a particle in random arrangement in a matrix is of large magnitude near a *point of contact* with another particle. These points of contact are necessarily well separated for particles

without sharp protuberances (as in the case of spherical particles). Batchelor et al. also proved analytically that the total heat flux across the part of surface of a particle that is near a contact point is determined by the local conditions and is large relative to the total flux across the parts of the surface *not* near a contact point. This effect is illustrated here using full-field numerical simulation of a three-dimensional microstructure using a hierarchical partition of unity meshless analysis procedure recently developed [24]. It is important to note that hierarchical partition of unity meshless analysis procedure employed here is devoid of any approximations. The code implementing this procedure is named jNURBS [20, 25 and 26]. Figure 7 shows the temperature and heat flux fields on the midsection of the TIM microstructure shown in Figure 4, obtained using jNURBS. Isothermal temperature boundary conditions were applied at the bottom (1 ^{o}C) and the top (0 ^{o}C) interfaces, and the other surfaces were subjected to adiabatic conditions. In all simulations presented in this paper, isothermal boundary conditions were assumed across the TIM in the direction of heat transfer, and the other surfaces were assumed to be adiabatic. Also, the interfacial thermal boundary resistance between the filler materials and the matrix was ignored.

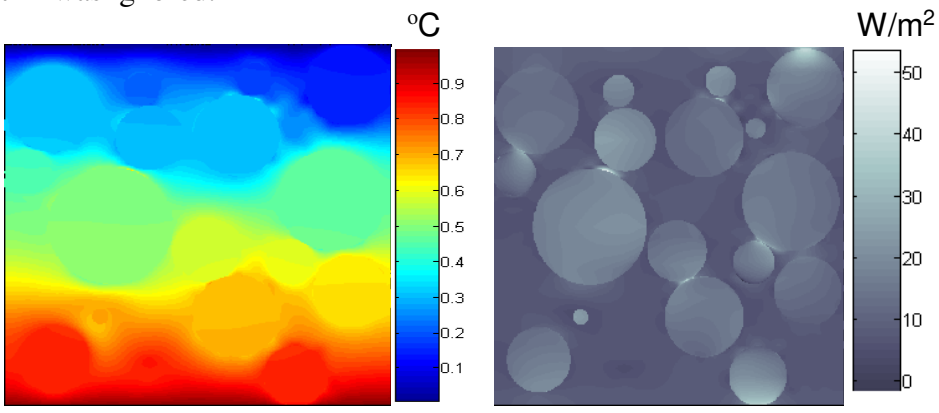

(a) (b)

Figure 7: (a) temperature and (b) heat flux fields obtained at the midplane of the microstructure (Figure 4) (y = 0.5) using jNURBS.

The heat flux contours in the image of Figure 7(b) show largest heat flux magnitudes at the *locations where particles are in near contact*. Batchelor et al. [23] proposed that the heat transported (in three-dimensions) *between* two spherical filler particles is approximately confined within a *cylindrical zone* of radius R_{12} shown in Figure 8 over which heat is transported between the particles (the axis of the cylinder is along the line joining the centers of the two spherical particles under consideration).

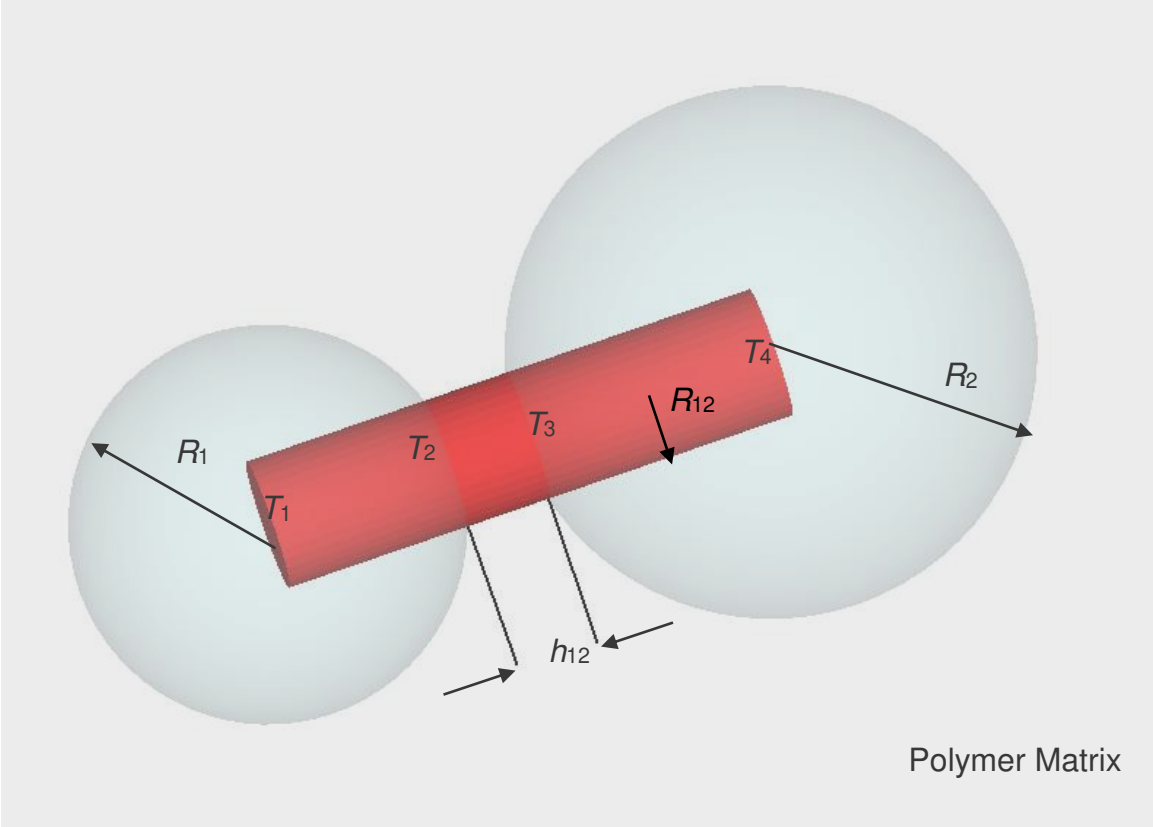

Figure 8: An illustration of the modeled cylindrical zone between two spherical particles embedded in the polymer matrix, through which the heat is transported.

Batchelor et al. [23] analytically estimated the conductance in the gap between two spherical particles as:

$$K_2 = \pi\, k_{\mathrm{m}}\, a_{12} \log\left(1 + \frac{{R_{12}}^2}{a_{12} h_{12}}\right) \tag{5}$$

where, K_2 is the inter-particle gap conductance, k_{m} is the embedded matrix thermal conductivity, R_{12} is the radius of the cylindrical zone mentioned earlier, and h_{12} is the minimum gap width between the filler particles as shown in Figure 8, and a_{12} is the mean radius of curvature of the two particles given by:

$$a_{12} = \frac{2R_1 R_2}{R_1 + R_2} \tag{6}$$

where, R_1 and R_2 are the radii of the spherical particles across which heat is transferred.

In the present study, we model the radius R_{12} of the cylindrical zone parametrically as:

$$R_{12} = \alpha\, a_{12} \tag{7}$$

where, α is an estimate of the fraction of the mean radius of curvature a_{12} defined earlier in Equation (6).

It is difficult to analytically model the heat transport in a spherical filler particle with non-uniform Neumann boundary conditions (as in the case of the spherical filler particles in the composite TIM system). Thus, it is difficult to arrive at an analytical expression for the equivalent conductance within a spherical filler particle. Therefore to model the heat transfer within a spherical filler particle, the cylindrical zones between the particles were extended *into* the particles. That is, the *cylindrical zones* were extended to the middle of each of the spherical particle, and the effective heat between the filler particles was assumed to conduct via these cylindrical zones. This is an approximation of the heat transfer *within* the spherical filler particles as heat would spread in all directions

within the spherical filler particle, but under *steady state* conditions, this may be a reasonable approximation. This is since the proposed model is equivalent to stating that the heat conveyed via these cylindrical zones is transferred to other spheres via other cylindrical zones in the particle. Thereby, the entire system of spherical particles is replaced by cylinders of different radii and lengths as shown in Figure 8 (the individual cylinder radius being dependent on the radii of the spherical particles across which the cylinder is placed as given by Equation (7), and the length of the cylinder being equal to distance between the centers of the two spherical filler particles). Thus, the conductances of the cylindrical zones within the spherical filler particles are evaluated as:

$$K_1 = \frac{k_p \, \pi \, R_{12}^{\,2}}{R_1} \tag{8}$$

$$K_3 = \frac{k_p \, \pi \, R_{12}^{\,2}}{R_2} \tag{9}$$

where, K_1 and K_3 are the conductances of the cylindrical zones within the spherical filler particles, k_p is the thermal conductivity of the filler particle, R_{12} is the cylindrical zone radius as defined in Equation (7) and R_1 and R_2 are the radii of the spherical filler particles as shown in Figure 8.

Therefore, combining Equations (5), (8) and (9), the effective conductance K_{12} between the centers of two spherical particles is estimated as:

$$K_{12} = \left[\frac{R_1}{k_p \, \pi \, R_{12}^{\,2}} + \frac{1}{\pi \, k_m \, a_{12} \log\left(1 + \frac{R_{12}^{\,2}}{a h_{12}}\right)} + \frac{R_2}{k_p \, \pi \, R_{12}^{\,2}} \right]^{-1} \tag{10}$$

There are two parameters that influence the outcome of the simulation. The first parameter, α, was defined in Equation (7).

The second parameter ε is related to the cutoff distance over which the interaction particle i with particle j is of relevance. The interaction is included in the network model if:

$$h_{ij} < \varepsilon \frac{2R_i R_j}{R_i + R_j} = \varepsilon\, a_{ij} \tag{11}$$

where, h_{ij} is the nearest gap between particles i and j, a_{ij} is the mean radius of curvature of the particles i and j, and interaction of particle i with the interface is included in the model if:

$$d_i < R_i + \varepsilon\left(2R_i\right) \tag{12}$$

where, d_i and R_i are the distance of the center of the filler particle from the interface and the radius of the filler particle respectively.

The java code [25] that generates the microstructure gives as output the radii and positions of the filler particles in the matrix, which are then used as inputs to the random network model. In addition to these, the thermal conductivities of the filler material and the polymer matrix, the top and bottom temperatures of the TIM (across which the heat is transported) and the parameters α and ε as described above are input to the code.

Given the input parameters, using the procedure described above, the contributions of the inter-particle conductances and the particle-substrate conductances are assembled into the global conductance matrix and solved for the nodal temperatures in the random network model. The code outputs the nodal temperatures by solving the

global conductance matrix. The heat flux entering/leaving the simulated TIM system is then calculated by considering the particles which are closer (as governed by Equation (12)) to the bottom/top interfaces of the TIM system. The bulk thermal conductivity value of the simulated TIM system is then evaluated using the Fourier's law of conduction. The network model was implemented and solved using MATLAB [27].

Results

Five different TIM formulations consisting of Alumina/Silver/Diamond fillers in Silicone/Epoxy matrices were used to validate the random network model. Random arrangements of filler particles in the matrix were generated (as shown in Figure 4) and the effective thermal conductivities of the composites were evaluated. The properties of the different polymer matrix–filler particle combinations used in the validation were:

i. Silicone matrix – (k_m = 0.2 W/mK), Alumina filler (k_p = 25 W/mK)

ii. Epoxy matrix – (k_m = 0.3 W/mK), Alumina filler (k_p = 25 W/mK)

iii. Silicone matrix – (k_m = 0.2 W/mK), Silver filler (k_p = 420 W/mK)

iv. Epoxy matrix – (k_m = 0.3 W/mK), Silver filler (k_p = 420 W/mK)

v. Silicone matrix – (k_m = 0.2 W/mK), Diamond filler (k_p = 2000 W/mK)

The temperature of the simulation cell at the bottom and the top interface was fixed at 1^{o}C and 0^{o}C respectively (since the assumed behavior is linear, the effective conductivity is independent of the specific temperatures input at the interfaces). As mentioned before, the other sides of the simulation cell were assumed to be adiabatic. Of the two parameters, α and ε described earlier, the parameter α has a direct influence on the accuracy since it is an integral part of the model to estimate inter-particle conductance. The parameter ε, on the other hand, influences the computational efficiency

since it is the means by which the dominant inter-particle interactions for a given particle are identified. Thus, while ε influences efficiency, its effect on accuracy is not expected to be significant. In the present study, the value of ε was estimated to be 0.5 based on the matrix exclusion probability distribution observed in Figure 5. This is since the probability of finding a spherical matrix region with a non-dimensionalized radius (r/r_{avg}) greater than 0.5 is less than 10% as seen from Figure 5. The parameter α was determined by tuning the random network model (RNM) result for *one* random microstructure to match with the result obtained using full-field numerical simulation of the *same* microstructure using jNURBS. Parameter value of α = 0.5 when used in the network model was found to produce results that best matched the effective conductivity obtained from the corresponding full field simulation. These values *were kept fixed in all the subsequent simulations*.

The temperatures obtained at the nodal points (the centers of the filler particles) using both the jNURBS and the RNM are compared in Figure 9 for two of the microstructures used in the simulations. This result allows one to compare the "*local*" temperature fields between the two solutions. In Figure 9, the axis represents the ratio of the radius of the filler particles (r_p) with respect to mean radius of all the filler particles in that particular microstructure (r_m), and the ordinate represents that ratio of the difference in temperatures obtained at the nodal points using jNURBS and RNM models, Δ, with respect to the applied temperature differential between the bottom, T_b, and top, T_t, interfaces of the microstructure. As can be seen from the results in Figure 9, the maximum difference observed between the calculated nodal temperatures using the two

models was within 10% of the magnitude of the applied temperature differential between the bottom (T_b) and top (T_t) interfaces of the microstructure.

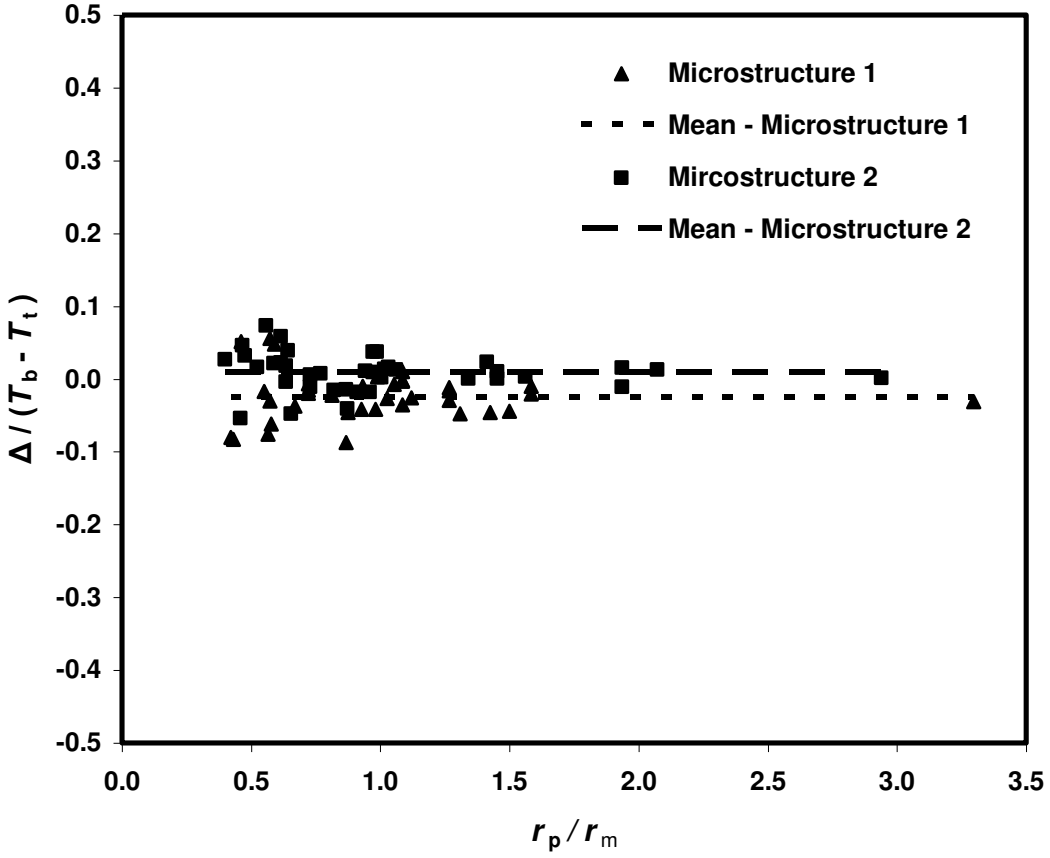

Figure 9: Relative difference of temperatures at the centers of the particles obtained using jNURBS and RNM.

One hundred simulations (considering twenty random microstructures of each matrix – particle combination) were performed in all, and the results are shown in Figure 10 and Table 2. As can be observed from the mean values of full-field and random network simulations, the difference in the mean values of effective thermal conductivity is at worst 5%, and in most cases significantly better than 5%. Also, from the plots we can clearly see that varying the conductivity of the base polymer matrix has a significant

effect on the bulk thermal conductivity of the composite TIM material in comparison to varying the conductivity of the embedded filler particles. For example, increasing the conductivity of the polymer matrix from 0.2 W/mK to 0.3 W/mK results in ~43% higher bulk TIM material composite conductivity whereas, increasing particle conductivity from 25 W/mK to 420 W/mK only results in ~14% higher bulk TIM material composite conductivity. Such design guidelines are critical to developing better TIMs.

The statistical significance of the simulation results were analyzed using the Student's t-tests. The results are tabulated in Table 3. The data in the table compare the effect of the following:

i. loading Alumina filler particles in Silicone and Epoxy matrices
ii. loading Silver filler particles in Silicone and Epoxy matrices
iii. loading Alumina and Silver filler particles in Silicone matrix and
iv. loading Alumina and Silver filler particles in Epoxy matrix

The results clearly show that there is a significant effect of varying the matrix conductivity (higher t-values of 20.51 and 19.28) on the effective composite thermal conductivity in comparison to that of varying the filler particle thermal conductivity (lower t-values of 6.90 and 9.34).

The t-tests were also performed to statistically quantify the difference between the effective thermal conductivity results of the full-field simulations and the RNM simulations for the twenty simulations for each of the five filler particle/matrix combinations mentioned above. A significance level of 95% was chosen for the t-tests. The statistically calculated t-values for each of the different polymer matrix–filler particle combinations used in the validation are tabulated in Table 4. The "critical" t-value (two-

tailed t-test) for all the five different filler particle-matrix combinations was 2.02. Since the statistically calculated t-value for all the five different filler particle-matrix combinations was less than the "critical" t-value, we can conclude that the "mean composite thermal conductivity values" of the full-field simulations and the RNM simulations are "*not significantly*" different with a 95% level of confidence. Finally, the run time of the RNM code (for a given microstructure) is a few seconds as compared to about four hours each of simulation time taken by the full-field simulations on a 3 GHz Pentium 4 machine with a 1GB RAM.

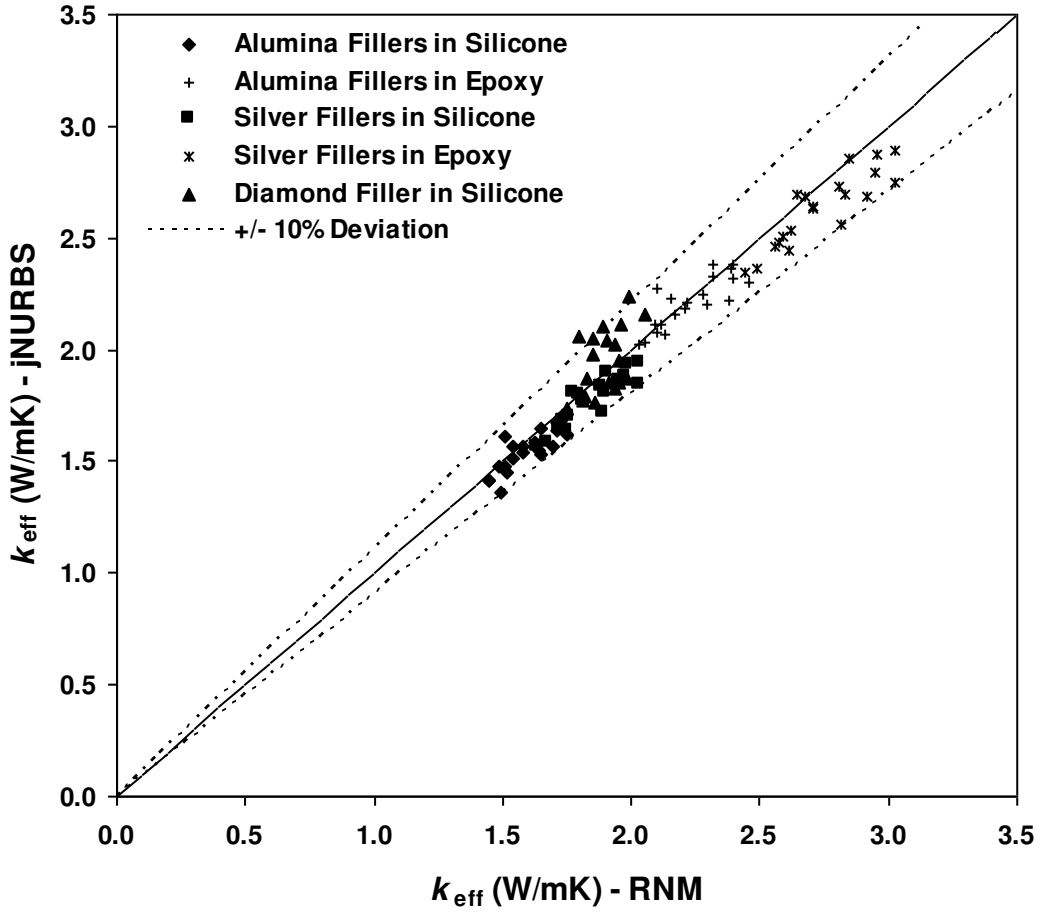

Figure 10: Comparison of effective thermal conductivities of random microstructures simulated using jNURBS and RNM.

Table 2: Comparison of effective thermal conductivities of the different filler particle – matrix systems simulated using jNURBS and RNM, and the analytical models.

Filler Particle - Matrix System	jNURBS (μ, σ) (W/mK)	RNM (μ, σ) (W/mK)	Maxwell Model (W/mK)	Rayleigh Model (W/mK)	BAM (R_b = 0) (W/mK)
Alumina - Silicone	(1.55, 0.09)	(1.58, 0.10)	0.98	1.16	2.70
Alumina - Epoxy	(2.21, 0.11)	(2.22, 0.13)	1.44	1.70	4.05
Silver - Silicone	(1.77, 0.11)	(1.83, 0.12)	1.03	1.23	2.70
Silver - Epoxy	(2.63, 0.16)	(2.73, 0.18)	1.54	1.85	4.05
Diamond - Silicone	(1.95, 0.15)	(1.90, 0.08)	1.03	1.24	2.70

Table 3: Statistical analysis of simulated filler particle-matrix combinations: t-test results

Filler Material	Polymer Matrix	Statistical t-value	Tabulated t-value	Significance Level	Comment
Alumina	Silicone	20.51	2.02	95%	"Significantly" different
	Epoxy				
Silver	Silicone	19.28			"Significantly" different
	Epoxy				
Alumina	Silicone	6.90			"Significantly" different
Silver					
Alumina	Epoxy	9.34			"Significantly" different
Silver					

Table 4: Comparison of RNM with jNURBS: t-test results

Filler Material	Polymer Matrix	Statistical t-value	Tabulated t-value	Significance Level	Comment
Alumina	Silicone	1.2	2.02	95%	Not "significantly" different
	Epoxy	0.08			
Silver	Silicone	1.57			
	Epoxy	1.75			
Diamond	Silicone	1.59			

Figure 11 depicts the significance of the contribution of the "*nearest*" neighbor interaction parameter of the RNM. The effect of decreasing the ε value from 0.5 to 0.1 is shown in Figure 11. Physically, this implies that the interaction zone of a "*test*" sphere with its neighbors is reduced by a factor of five. As seen from the Figure 11, the mean values are nearly the same between the two cases. The simulation results were analyzed statistically using t-tests as before. The statistically calculated t-value for Alumina fillers in Silicone matrix was 1.29 and for Alumina fillers in Epoxy matrix was 1.43. Since both the t-values are less than the critical t-value of 2.04, we can conclude that the simulations are "*not significantly*" different with a 95% level of confidence. This confirms the important result proposed by Batchelor et al. [23] that bulk of the heat in particulate composites consisting of highly conducting filler particles is transported via the "*nearest*" neighbors.

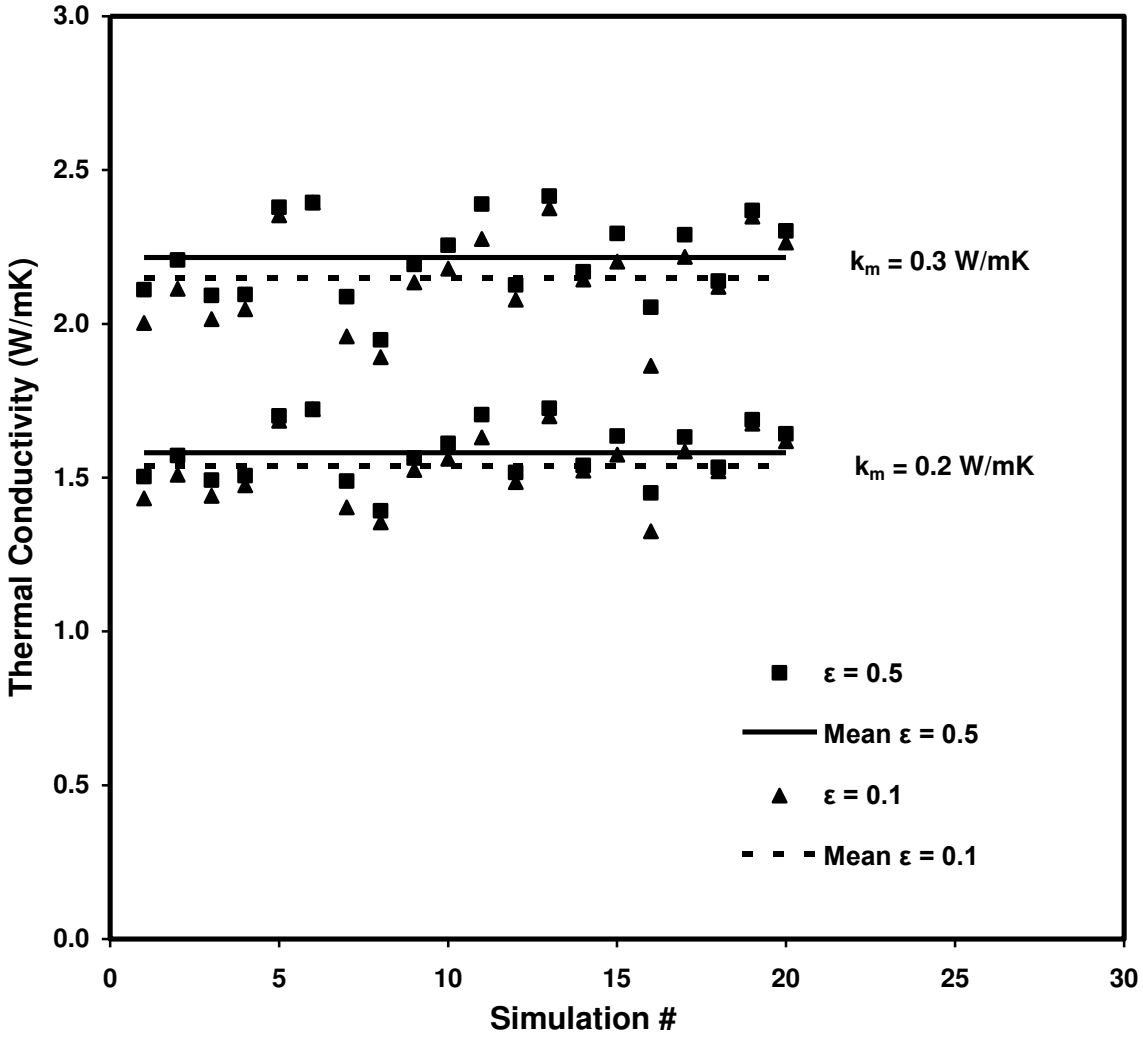

Figure 11: Effect of ε on the network model simulations for Alumina fillers loaded into Epoxy and Silicone matrices, respectively.

Experimental Microstructure Simulations

Fifteen microstructures with 58% filler volume loading were generated using the experimental particle size distribution data for Alumina particles shown in Figure 2. The matrix material was assumed to be Silicone for comparison to the experimental measurements. The size (diameter) of the filler particles was limited to between 5 -15 μm as shown in

Figure 12 below, to generate microstructures with computationally manageable total number of particles. In the scenario when smaller sized particles are considered, the total number of particles in the microstructure increased tremendously. Similarly, as larger sized particles were considered, the total size of the RVE had to be increased to fit the larger sized particles, which in turn increased the total number of particles. Therefore, the size (diameter) of the particles was limited to between 5-15 µm. The size of the RVE considered was 60 µm x 60 µm x 60 µm (the RVE side being four times the maximum particle size). The total number of particles simulated in each RVE was 12,582. An illustration of the simulated microstructures is shown below in Figure 12.

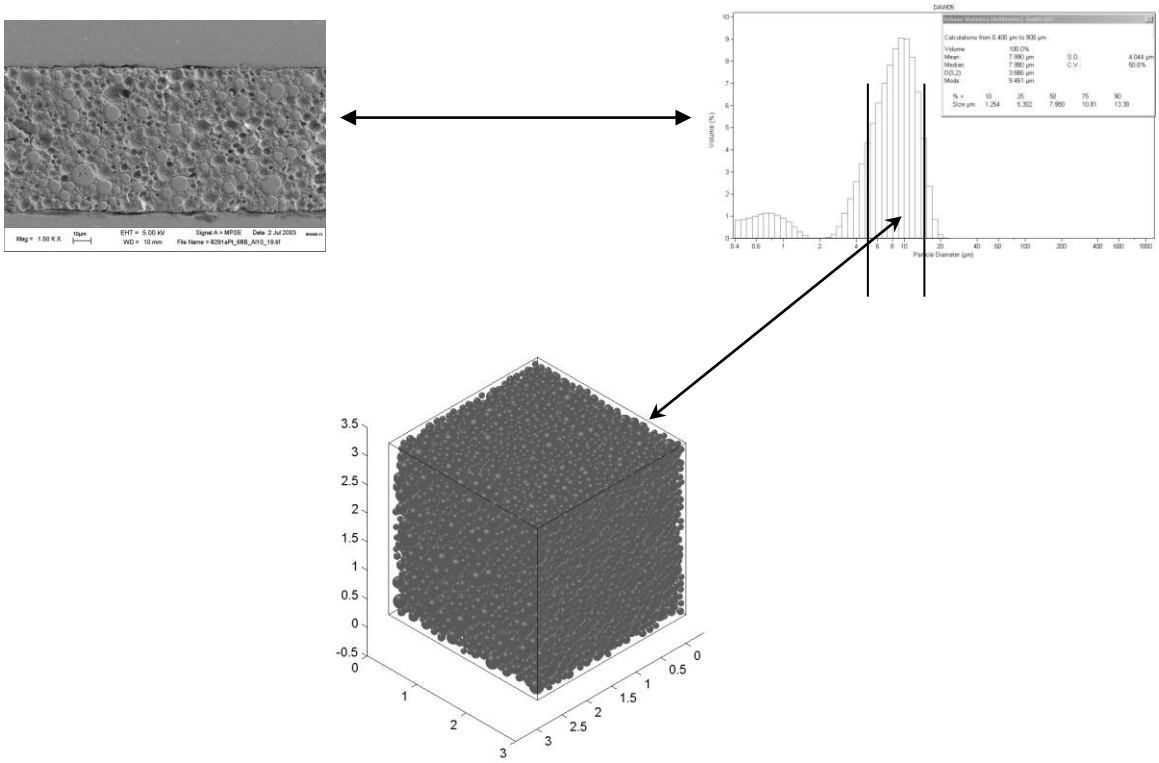

Figure 12: Experimental microstructure RVE's.

The results of the simulations are shown below in Figure 13. The mean thermal conductivities of the network model simulations matched to within ~15% of the

experimentally measured values. The mean runtime for each of the simulation shown below in Figure 13 was ~60 hrs on a on a 3 GHz Pentium 4 machine with 1GB RAM. The network model always predicted lower thermal conductivity values in comparison to the experiments. The primary reason for the difference is related to the microstructural characteristics of the simulated and the experimental microstructures. In general, the average matrix region size between particles as measured by the matrix exclusion probability was larger in the simulated microstructures relative to the experimental microstructures. This appears to correlate with observed difference in effective conductivity.

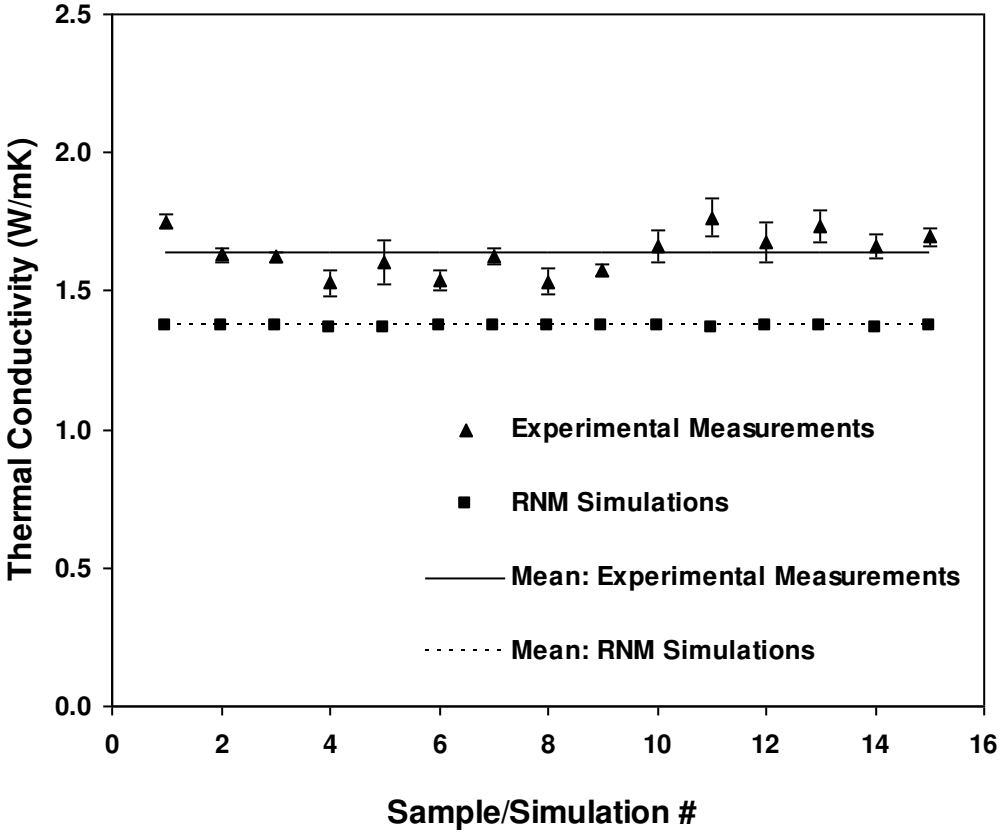

Figure 13: Comparison of simulation of realistic microstructures to the experimental measurements for Alumina particles loaded in Silicone matrix.

Conclusions

A random network model was developed and applied to evaluate the effective thermal conductivity of particulate thermal interface materials. The heat transport between the filler particles was accurately captured by implementing Batchelor's estimate of conductance between two spherical particles in near contact. This enabled the random network model to account for inter-particle interaction. The heat conducted within the spherical filler particles was approximated by cylindrical zones. The network model was used to evaluate the bulk conductivities of random microstructures. The results obtained using the random network model are in very good agreement (within 5%) with the results of the full field simulations (jNURBS) of identical microstructures. The simulations presented here are both efficient (since they required two orders of magnitude smaller computation time to complete in comparison to the full field simulation) and accurate. The simulations carried out using the model indicate that improving matrix conductivity has a far greater impact than improving particle conductivity on the effective conductivity of high-contrast composites. This result has significance to nanostructured composites that aim to improve effective conductivity by randomly mixing highly conducting nanotubes.

Ongoing efforts are directed towards extending the network model to systematically study the effect of polydispersivity of the partices on the effective behavior. Effort is also on to efficiently perform system level simulations that include the processor and heat spreader interfaces with their associated matrix-rich regions in addition to the bulk material.

Acknowledgements

This work was partially supported by the General Electric Corporation as part of a U.S. Department of Commerce, Advanced Technology Program, Cooperative Agreement Number 70NANB2H3034. The authors also acknowledge the financial support from members of the Cooling Technology Research Center, a NSF IUCRC at Purdue University.

Reference

1. Maxwell, J. C., *Electricity and Magnetism*, 1st ed. (Clarendon, Oxford, 1873).

2. Lord Rayleigh., "On the Influence of Obstacles Arranged in Rectangular Order upon the Properties of a Medium", *Phil. Mag.,* Vol. 34, pp. 481-502.

3. Torquato, S., Random Heterogeneous Materials, Springer-Verlag (New York, 2002).

4. McPhedran, R. C. and McKenzie, D. R., "The Conductivity of Lattices of Spheres. I. The Simple Cubic Lattice", *Proc. R. Soc. Lond. A.*, Vol. 359, pp. 45-63, 1978.

5. McKenzie, D. R., McPhedran, R. C. and Derrick, G. H., "The Conductivity of Lattices of Spheres. II. The Body Centered and Face Centered Cubic Lattices", *Proc. R. Soc. Lond. A.*, Vol. 362, pp. 211-232, 1978.

6. Gu, G., Liu, Z., 1992, "Effects of Contact Resistance on the Thermal Conductivity of Composite Media with a Periodic Structure," *Journal of Physics D: Applied Physics*, Vol. 25, pp. 249-255.

7. Hasselman, D. P. H., Johnson, L. F., "Effective Thermal Conductivity of Composites with Interfacial Thermal Barrier Resistance", *J. Compos. Mater*., Vol. 21, pp. 508-515, 1987.

8. Nan, C. W., Birringer, R., Clarke, D. R., Gleiter, H., "Effective Thermal Conductivity of Particulate Composites with Interfacial Thermal Resistance", *J. Appl. Phys*., Vol. 81, no. 10, pp. 6692-6699, 1997.

9. Benvensite, Y., "Effective Thermal Conductivity of Composites with a Thermal Contact Resistance between the Constituents: Non-dilute case", *J. Appl. Phys*., Vol. 61, no. 8, pp. 2840-2843, 1987.

10. Bruggeman, D., "Berechnung verschiedener physikalischer Konstanten von heterogenen Substanzen", *Ann. Physik (Liepzig)*, Vol. 24, pp. 636-679, 1935.

11. Landauer, R., "The Electrical Resistance of Binary Metallic Mixtures", *J. Appl. Phys.,* Vol. 23, pp. 779-784, 1952.

12. Landauer, R., "Electrical Conductivity in Inhomogeneous Media", Electrical, Transport and Optical Properties of Inhomogeneous Media, J. C. Garland and D. B. Tanner (eds.), AIP, New York, pp. 2-43, 1978.

13. Every, A. G., Tzou, Y., Hasselman, D. P. H., Raj, R., "The Effect of Particle Size on the Thermal Conductivity of ZnS/Diamond Composites", *Acta Metall. Mater*., Vol. 40, 1992.

14. Kanuparthi, S., Zhang, X., Subbarayan, G., Sammakia, B. G., Gowda, A. and Tonapi, S., "Full-Field Simulations of Particulate Thermal Interface Materials: Separating the

Effects of Random Distribution from Interfacial Resistance", *Proc. of Itherm'06*, San Diego, May 30 – Jun 2, 2006.

15. Kanuparthi, S., Zhang, X., Subbarayan, G., Siegmund, T., Sammakia, B. G., Gowda, A. and Tonapi, S., "Random Network Percolation Model for Particulate Thermal Interface Materials," In Proceedings of the 10th Intersociety Conference on Thermal and Thermomechanical Phenomena in Electronic Systems (Itherm 2006), IEEE.

16. Devpura, A., Phelan, P. E. and Prasher, R. S., "Percolation Theory Applied to the Analysis of Thermal Interface Materials in Flip-Chip Technology", *Proc. of ITHERM*, Vol. 1, pp. 21-28, May 23-26, 2000.

17. Devpura, A., P. E. Phelan, and R. S. Prasher, "Percolation Theory Applied to Study the Effect of Shape and Size of the Filler Particles in Thermal Interface Materials", *Proc. ASME Heat Transfer Division*, Vol. 366(4), pp. 365–371, 2000.

18. Devpura, A., Phelan, P. E., and Prasher, R. S., ''Size Effects on the Thermal Conductivity of Polymers Laden With Highly Conductive Filler Particles'', *Microscale Thermophys. Eng.*, Vol. 5(3), pp. 177–189, 2001.

19. Zhang, X., Kanuparthi, S., Subbarayan, G., Sammakia, B. G., and Tonapi, S., "Hierarchical Modeling and Trade-Off Studies in Design of Thermal Interface Materials", *Proc. of ASME, InterPACK'05*, San Francisco, July 17-22.

20. Kanuparthi, S., Zhang, X., Rayasam, M., Subbarayan, G., Sammakia, B. G., Gowda, A., and Tonapi, S., "Hierarchical Design of Thermal Interface Materials", *ICCES'05 Conference*, India, December 1-6, 2005.

21. Santiso, E., and Muller, E. A., "Dense Packing of Binary and Polydisperse Hard Spheres," *Molecular Physics*, Vol. 100, No. 15, pp. 2461-2469, 2002.

22. Lu, B., and Torquato, S., "Nearest-Surface Distribution Functions for Polydispersed Particle Systems," *Physical Review A*, Vol. 45, No. 8 (1992), pp. 5530-5544.

23. Batchelor, G. K. and O'Brien, R. W., "Thermal or Electrical Conduction through a Granular Material", *Proceedings of the Royal Society of London. Series A, Mathematical and Physical Sciences*, Vol. 355, No. 1682, 313-333, 1977.

24. Rayasam, M., Srinivasan, V. and Subbarayan, G., "CAD Inspired Hierarchical Partition of Unity Constructions for NURBS-based, Meshless Design, Analysis and Optimization," *International Journal for Numerical Methods in Engineering*, Accepted.

25. Zhang, X. "Constructive Modeling Strategies and Implementation Frameworks for Hierarchical Synthesis." Ph.D. Thesis, Purdue University, 2004.

26. Zhang, X. and Subbarayan, G., "jNURBS: An Extensible Symbolic Object-Oriented Framework for Integrated Mesh-less Analysis and Optimal Design", *Advances in Engineering Software*, Vol. 37, No. 5, 287-311, 2006.

27. MATLAB: a registered trademark of The Mathworks, Inc., Natick, MA.

Author Biographies:

Dr. Sasanka Kanuparthi is a Senior Engineer at Amkor Technology. He received his Bachelors in Technology in Chemical Engineering from Indian Institute of Technology, Chennai, India in 2000. He received his Masters and Doctorate in Mechanical Engineering from Purdue University in 2002 and 2007, respectively. His research interests include Experimental and Computational Heat Transfer, Thermal Management of Microelectronics, Design of Thermal Systems and Design of Nano-composites.

Dr. Ganesh Subbarayan is a Professor of Mechanical Engineering at Purdue University. He was previously at University of Colorado (1994-2002) and at IBM Corporation (1990-1993). He holds a B.Tech degree in Mechanical Engineering (1985) from the Indian Institute of Technology, Madras and a Ph. D. (1991, direct PhD program) degree in Mechanical Engineering from Cornell University. Dr. Subbarayan's research is in Computational Modeling and Design of objects over multiple length scales with applications to reliability of Microelectronic Interconnects and Packages. Dr. Subbarayan is a recipient of the 2005 Mechanics Award from the ASME EPP Division, 2005 University Faculty Scholar Award from Purdue University, NSF CAREER award, the NSF Research Initiation Award, the 2003 Charles E. Ives Outstanding Paper Award from the Journal of Imaging Science and Technology, the 2002 Highly Commended Award from Soldering and Surface Mount Technology journal, the Itherm 2000 Best Paper

Award, the 1996 Peter A. Engel Best Paper Award from ASME Journal of Electronic Packaging, and an IBM Invention Achievement Award. He has served on the program committees of several conferences including the ASME/Pacific Rim International Intersociety Conferences on Electronics Packaging (1997 program co-chair, 1999 reliability track chair, 2001 Modeling and Characterization track chair), ASME International Mechanical Engineering Conference and Exhibition (2002 Program Chair, EPP Division) and Intersociety Conference on Thermal and Thermomechanical Phenomenon in Electronic Systems (2002 program co-chair, Mechanics). He is a Fellow of ASME and he currently serves as the Editor-in-Chief of IEEE Transactions on Advanced Packaging.

Dr. Thomas Siegmund is Professor of Mechanical Engineering at Purdue University. He holds a Diplom Ingenieur (1990) and Doctorate (1994) from the University of Leoben, Austria. His research interests are in computational solid mechanics, biomechanics and manufacturing systems. Dr. Siegmund is a Purdue University Faculty Scholar (2004), a recipient of the 2002 Best Paper Award of the American Society of Composites. From 1997-1999 he was a Lecturer of the Federation of European Materials Societies (FEMS), and from 1995-1996 a recipient of the Erwin Schrödinger Fellowship, Austrian Science Foundation. He contributed to the organizational structure of several conferences including the 2008 International Congress of Technical and Applied Mechanics, the 2006 and 2008 Annual Technical Meetings of the Society of Engineering Science, and has been a lecturer at the International Center Mechanical Sciences (CISM) in Udine, Italy.

Dr. Bahgat Sammakia is Director of the Integrated Electronics Engineering Center. Bahgat Sammakia received his Bachelor of Science degree in Mechanical Engineering in 1977, from the University of Alexandria in Egypt. He received the masters and doctorate degrees in mechanical engineering in 1980 and 82 respectively from the State University of New York at Buffalo. His research work was in the areas of natural convection heat transfer. After graduating from SUNY, Bahgat worked at the University of Pennsylvania as a postdoctoral fellow.

Bahgat joined IBM in 1984 as an engineer in the thermal management area. In 1985 he was promoted to manager of the thermal management department. Bahgat continued to work in IBM until 1998, in various management positions, including managing the thermal and mechanical analysis groups, the surface science group, the chemical lab, the site technical assurance group, and his last position in IBM was manager of development for organic packaging in the IBM Microelectronics division.

Bahgat holds seven US patents and twelve IBM technical disclosures; he has published over 50 technical papers in refereed journals and conference proceedings. Bahgat has contributed to three books on natural convection heat transfer and electronic packaging.